

## Enhancement of PAPR Abatement for FBMC System

Kanagaraj Venusamy<sup>1</sup>, Malarvizhi Muthuramalingam<sup>2</sup>, S. Kannadhasan<sup>3</sup>, R. Vanithamani<sup>4</sup>

Submitted: 28/10/2022

Revised: 16/12/2022

Accepted: 03/01/2023

**Abstract:** Even though FBMC is a candidate waveform for fifth generation technology, it has major drawbacks that high PAPR (Peak to Power Average Ratio) which causes nonlinearity in power amplifiers and cost inefficiency. It also leads to signal degradation and results in harmonics. Therefore, much method has been used to reduce Peak power of filter bank multicarrier system. In this paper detailed analysis of effect of PAPR in multicarrier system and gradual improvement of PAPR reduction is discussed. Particularly effects of DFT (discrete Fourier Transform) spread, optimum phase condition terms and in addition to that pruned input with one tap scaling is discussed. From this technique starting from simple DFT spread, DFT with phase condition and DFT with precoding offers good reduction in square of crest factor in step-by-step manner than traditional FBMC. Despite not bearing a cyclic prefix, they anticipate lower off-putting discharge. Finally, these schemes are compared in terms of Complexity, rate of error in bits and higher peak power with respect to average to find the optimum one with same properties of conventional FBMC.

**Keywords:** FBMC, Precoding matrix, Pruned DFT spread, Hermite filters, Optimum phase shift

### 1. Introduction

Evaluation of the multicarrier system leads to development of fast-growing technology connecting anyone from any part of the world. The OFDM fashion with a cyclic prefix that uses a class of quadratic subcarriers is the wide case anticipated for dependable connectivity. But due the presence of cyclic prefix, less time and frequency synchronization, poor Out of Band Emission leads to innovation of FBMC. Filter Bank Multicarrier system is a new multi carrier waveform with bank of filters that delivers better spectral shaping subcarriers than OFDM. Lack of CP can be evened by designing prototype sludge by dwindling hindrance among subcarriers. And also by Engaging Amplitude Modulation that balances both in phase and quadrature counterbalance (OQAM), as much of communicated information can be attained. It put backs the perpendicular state of imaginary section with the alleviation in real quadratic condition. This seed to natural hindrance, focusing on the complex part, which makes path assessment and Multiple- Input and Multiple- Affair (MIMO) more grueling. Besides the conversion of analog and digital converter and abridged transmit signal effect on booster amplifiers is a great threat in real-time scenario for the reason that demolish the exceptional frequency captivity of FBMC. High nonlinearities also produce

distortion in channel estimation due to distortion in transmitted signal. To overcome many methods have been proposed. Firstly, the addition of DFT just reduce the peak power to marginal value. Secondly the addition of phase shift to DFT tolerates high PAPR. Not only the phase term four different version of optimum phase shift pattern is used which are generated with help of switch bits. addition Finally a novel reduction scheme which is extension of DFT spread of pruned input in combination with one tap scaling retains all the basic properties of conventional FBMC such as low OOB emission, low latency, high spectral efficiency and provides less PAPR. Due modifications are done by replacing the complex to real transformation to Pruned DFT with one tap scaling to make power constant. Designing a precoding DFT matrix and making it spread with input. Further spread in frequency instead of time modified which employs a modified prototype filter. Finally, we compare various methods of reduction with the conventional method and observe the results obtained.

### 2. Related Work

From time-to-time research on FBMC is still on due to nature of high spectral shaping and less OOB. There are many reduction techniques are available to reduce the crest power to norm power ratio. The effects high peak power in channel estimation problem is tolerated by interference cancellation method with PAPR reduction [2] failed in achieving high success. Using Companding coding Output of IFFT is copied to overlapping factor and the passed through prototype filter. Finally, the overlap sum is added at the output. In FBMC OQAM with simple DFT spreading two additional blocks are used .one is called as original block and another one is reverse block where the input symbols are reversed. Then it follows IFFT and filter which was discussed in [3].The development of optical communication due to its high

*1 Assistant Professor (SG), Department of Mechatronics, Rajalakshmi Engineering College, Thandalam, Chennai.  
kanagaraj.v@rajalakshmi.edu.in*

*2 Department of Communication Systems, College of Engineering, Chennai, Tamilnadu, India, malarvizhibh9903@gmail.com*

*3Department of Electronics and Communication Engineering, Study World College of Engineering, Coimbatore, Tamilnadu, India, kannadhasan.eca@gmail.com*

*4 Department of Biomedical Instrumentation Engineering, Avinashilingam Institute for Home Science and Higher Education for Women, Coimbatore, Tamilnadu, India, vanithamani\_bmie@avinut.ac.in*

speed applications requires DSP as a transceiver system. Therefore, the efficiency of different modulation schemes is compared by S. Alshami[4] and same as the analysis of FBMC[16] in single side banded system for optical communication is discussed by X. Zhang *et al*[5].The comparison of uplink performance with FBMC and OFDM with carrier and timing offset plot is discussed in [6].The new series of vectors are designed for conversion and then multiplied by cyclic shift pattern to reduce PAPR [7]. But it has high computational complexity. Design of filter banks are the major part of concern in FBMC system. In paper[8] the implementation of FBMC using modified Bartlett-Hanning, Root raised cosine pulse (RRC),and other modified impulses including traditional PHYDYAS and Hermite, are discussed with Multiple input FBMC system. The paper [9] is the extension of conventional PTS system where the single layer is divided into blocks and multiplied by optimum phase factor which is determined by genetic manner based consensual biased transmit sequence algorithm leads to reduction only about ~3 dB than conventional method. The conventional PTS and DFT based PTS are simulated in [10]. A process with many iterations using kernel functions named tone reservation results in mathematical intricacy where as General DFT spreading-reduce significantly than DFT [12]. Theoretical analysis of discrete Fourier transform and its mathematical calculations were analyzed in [14]. In an identically time shifted multicarrier (ITSM) algorithm four phase shift pattern has been proposed and multiplied with the IFFT output to shift the peak power and to maximize the amount of PAPR ratio [17]. In Section III quick review of conventional FBMC is described with transmission system model. The effects of high PAPR in power amplifier are also discussed. Then enhancement of PAPR reduction from DFT spread to pruned DFT method is then presented with its mathematical descriptions in fourth Section. Eventually, in Section V we present counterfeit effects of the PAPR and the error rate performances (BER) of proposed styles in fading channel.

### 3. Outline of FBMC OQAM

Spectral leakages of sinc function and continuous addition of multiple carriers in OFDM leads to large crest power PAPR and unwanted discharge in frequency respectively. Thus multiple carrier system with presence of filter fashion prevails the restriction of Frequency Division of orthogonal Multicarrier by adding common shaping pollutants which deliver a well-dissected surrogate medium in both time and frequency realms. Besides it abbreviates equalization in the of shortage Cyclic Prefix. Further FBMC systems holds spectral constrained waves by engaging counterbalance Quartet Amplitude Modulation (i.e OQAM), similar that real and imaginary shifted in half the symbol period to give full bandwidth capacity in FBMC systems. The main difference with OFDM is the presence of sludge banks on the transmitter and by the analysis sludge bank (AFB) in the place of FFT plus CP out on the receiver. In Figure 1 it is observed that the sludge banks correspond of an assemble of fringe of pollutants that summons N signals inputs to give N resultants. In Figure 1 the sludge bank used at the transmitter side is called the conflation sludge bank and the sludge bank used on the receiver side is

called the analysis sludge bank. The resembling form of input signal is attained from periodical to resembling motor and also passed through conflation sludge bank. Now the affair of conflation sludge is back to periodical form. On the receiver side rear process of transmitter happens. This fully packed architecture is referred as transmultiplexer or TMUX.

#### 3.1 System Architecture

The main processing blocks of the FBMC Transmultiplexer (TMUX) correspond of OQAM initialization, conflation sludge bank, the investigation (analysis) sludgebank, and the OQAM de-duping.

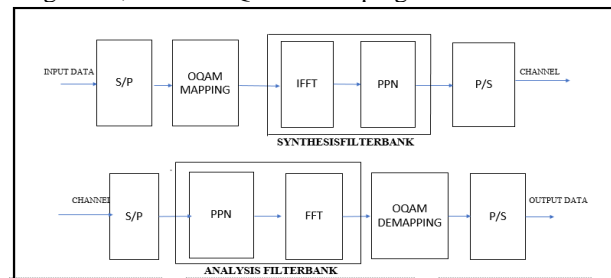


**Fig.1.** Schematic of FBMC

OQAM initialization and termination block has two functions, foremost operation is complex-to-real transfiguration, where the absolute and unreal corridor of complex-valued symbols are isolated to setup pair of altered symbols. It also escalates the Nyquist rate by 2. By phase staggering styles the imaginary symbol lags the real value whereas not in the case of QAM modulation. and the term 'neutralize' reflects the counteract partial shift in time between the absolute and the unreal part of a complex symbol. Synthesis Filter Bank consists of equal number of conflation pollutants and samplers as that of subcarriers and its vice versa at the reception.

The zero frequency carrier initial filter in the filter bank association is called prototype filter where the other filter members are derived by linear phase shift of it. The sludge portions are multiplied by  $e^{j\pi 2k/M}$ , that corresponds to dislocation of FFT by  $k/M$  of the frequency response. When all the FFT labors are considered, a filters of M fringes are attained, in which  $1/M$  multiple of real value is on the frequency axis. Only at the zero crossing which is  $1/M$  of integer multiples proves the orthogonality condition and appears as non-zero by base of Nyquist palpitation shaping. In this work, the better prototype sludge is designed with the lapping factor  $K = 4$  where K is an integer number as lapping occurs in time sphere and addition of measure in frequency sphere independently [22].

#### 3.2 Effect of high PAPR in power amplifier:

Being a multicarrier system with all these advantages of low OOB emission, higher bandwidth, multiuser facility high peak to power average is a significant drawback. From OFDM in 4G to FBMC in 5G, this PAPR affects the efficiency of power amplifier. Let us make clear how it affects in band and out from band effect of the signal. Firstly, Peak to power average ratio is defined as ratio of highest crest power or the instantaneous rate at which energy is flowing across some defined boundary to mean power or averaged over some specified period of time. Due to effect the high input power system

like Power amplifier, filters, fiber cable, channel becomes nonlinear. If the output frequency components of the transmitting signal are not in proper proportion leads to amplitude distortion [1]. This nonlinearity in Power amplifier makes the signal saturate. Thus to make them in linear region again, either back off should be high or the input biasing should be high than the necessary. It creates lesser battery lifetime and makes the components damage. On the other hand, excess amplification, or attenuation result in certain range of unwanted frequency in the given range of signal. So the output spectrum spread beyond input spectrum (i.e) new frequency component are produced outside the given input frequency and also new frequency component are added within frequency band which overlap and produces integral multiple of fundamental frequency leads to intermodulation distortion. Therefore, mandatory measures should be taken to reduce PAPR in FBMC.

#### 4. Enhancement of PAPR Reduction

##### 4.1 DFT based reduction:

The effect of IFFT in analysis filter bank of FBMC leads to high PAPR due to addition of QAM symbol on subcarriers at different time instants. Therefore, a method should be involved to tolerate the IFFT. Hence as like SCFDMA which is nothing but addition of DFT spread with cyclic prefix and subcarrier allocation, DFT block is added with IFFT in FBMC. The input symbols are mapped on  $M_s$  sub channel of DFT where frequency domain of given sequence is obtained. Then IFFT of the respective frequency domain is done, which cancels the effect of added symbols. This idea is very simple and less complex and also it reduces PAPR of conventional FBMC. Many methods are detected from these DFT spread technique.

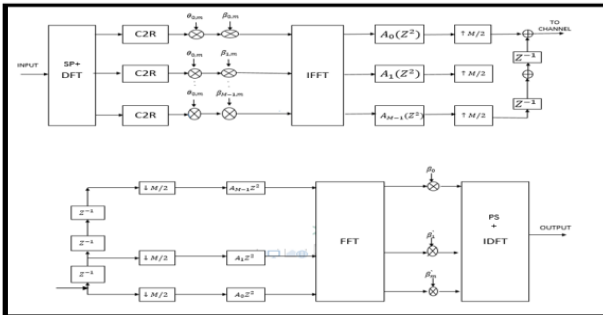


Fig. 2. Block diagram of DFT spread FBMC

##### 4.2 DFT spread with optimum phase shift:

Two signals of same phase get added in amplitude and result in signal with high amplitude which we termed as constructive interference. Similarly signals of different phase result in subtraction of amplitude. Therefore, if there is a phase shift between transmitted symbols, the resulting output will be less than the peak power. This idea leads to the method of reduction named time shift with DFT spread.

##### A. System architecture:

System efficiency depends on three main blocks: switch bit block, DFT spread, phase shift factor. Firstly, the input sequence is divided into blocks and not directly passed

through IFFT instead they are converted into frequency domain by DFT operation. This is to cancel the effect of QAM symbol on IFFT mapping. Then, real and imaginary are separated according to the subcarrier index. Then element wise multiplication of real and imaginary term with their phase shift pattern is done respectively. These phase shift patterns are designed in such a way leading to effect of single carrier system. Followed by IFFT shift and it is circularly shifted based on the property of cyclic time shift sequence of multiplying by  $e^{\frac{j2\pi kn}{N}}$ . This is done using toggle bit one where the odd index was in the opposite polarity of the even index. As a result waveform  $x_l^{(1)}(t)$  and  $x_l^{(2)}(t)$  are generated. Then to avoid spectral leakages IFFT are copied, overlapped and added.

The optimum phase shift scheme used are [17]

$$\alpha_{n,m} = (-1)^{m+j^n}$$

$$\mu_{n,m} = (-1)^m j (-j)^n \quad (1)$$

$$\alpha_{n,m} = (-1)^m (-j)^n$$

$$\mu_{n,m} = (-1)^m j^{n+1} \quad (2)$$

Where  $m=0,1,\dots,M-1$  and  $n=0,1,\dots,N-1$ [17]

Now after passing the above input in toggle bit  $2, x_l^{(3)}(t)$  and  $x_l^{(4)}(t)$  are generated. It is inferring from these pattern that the symbols that are on the same carrier are differed in polarity and symbols on different subcarrier are  $90^\circ$  phase shift of each other. Of these four version  $x_l^{(1)}(t)$  and  $x_l^{(2)}(t)$  are differed in phase shift with half bit delay in imaginary part where as  $x_l^{(3)}(t)$  and  $x_l^{(4)}(t)$  have same phase shift of  $x_l^{(1)}(t)$  and  $x_l^{(2)}(t)$  respectively but delayed in real part. To tolerate this real part delay  $j$  is multiplied by means of conditional multiplier. Of the above four versions, the one with minimum peak power is selected. Procedure is continued for all  $l$  blocks and concatenated with previous block. Thus both real and imaginary are identically shifted in phase in spite of shift in time.

##### B. Mathematical Representation:

Let  $A_{n,m}$  and  $B_{n,m}$  be DFT output of absolute and quadrature part,  $u$  be the number of blocks separated  $V$  be the number of FBMC symbol in each block, thus the four version of phase shifted waveform are:

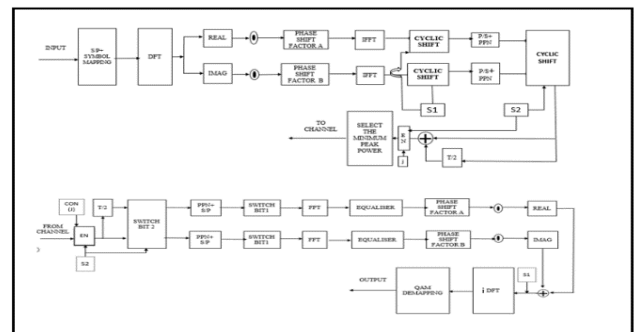


Fig.3. Block diagram of DFT spread with optimum phase shift FBMC

$$x_l^{(1)}(t) = \sum_{n=0}^{N-1} \sum_{m=uv}^{(u+1)V-1} (-1)^m \left\{ A_{n,m} p(t - mT) + j B_{n,m} p(t - mT - \frac{T}{2}) e^{j\pi \frac{2\pi(t+\frac{T}{4})}{T}} \right\} \quad (3)$$

$$x_l^{(2)}(t) = \sum_{n=0}^{N-1} \sum_{m=uv}^{(u+1)V-1} (-1)^m \left\{ A_{n,m} p(t - mT) + j B_{n,m} p\left(t - mT - \frac{T}{2}\right) e^{jn \frac{2\pi(t-\frac{T}{4})}{T}} \right\} \quad (4)$$

$$x_l^{(3)}(t) = \sum_{n=0}^{N-1} \sum_{m=uv}^{(u+1)V-1} (-1)^m \left\{ j A_{n,m} p\left(t - mT - \frac{T}{2}\right) - B_{n,m} p(t - mT) e^{jn \frac{2\pi(t+\frac{T}{4})}{T}} \right\} \quad (5)$$

$$x_l^{(4)}(t) = \sum_{n=0}^{N-1} \sum_{m=uv}^{(u+1)V-1} (-1)^m \left\{ j A_{n,m} p\left(t - mT - \frac{T}{2}\right) - B_{n,m} p(t - mT) e^{jn \frac{2\pi(t-\frac{T}{4})}{T}} \right\} \quad (6)$$

#### 4.3 Pruned DFT precoding method:

Principle of using DFT with addition to precoding in process of bringing down the crest power leads to idea of introducing method called Pruned DFT precoding. Usually, precoding is used on the receiver to know the prior knowledge of the transmitted information. In this method, precoding is used in the transmitter itself to design the system with low peak value. Thus the precoding matrix plays the vital role in reduction. It has information of filtered pulse vector either PAM or QAM with linear phase shift and spreading matrix. Also to help in recovery of transmitted signal at exact sampling time at the receiver Hermite filter with Hermite polynomials are used. Lower peak effect, lower spectral losses, lower communication delay with lower computational complexity are the advantages of pruned DFT method with precoding. The performance of the system in multipath fading channel especially doubly selective channel is also notable. The effect of mapping on half the symbol carrier is tolerated by reducing time frequency spacing to 1.5.

#### A. System architecture:

system efficiency depends primarily on the precoding block and Hermite filter block. Initially, the half input of subcarriers is used for mapping instead of full frequency carrier to reduce the column effect. The DFT matrix of the same size as that of the subcarriers is created to spread the symbols therein. Then considering the highest diagonal element along with the pulse matrix is determined to equalize the peak value of spreading matrix. Finally, with this calculated matrix, a scaling factor to make constant power is found and then multiplied with the half QAM symbol. All these together constitute the pruning precoding matrix. Since the channel with known RMS delay and delay spread is considered, precoding is easier in this case. Hermite filters which are developed from the Gaussian filter with zero mean that is used for quantum analysis replaced instead of PHYDAS of traditional FBMC. Using Hermite helps us to identify signals whose edge is at least greater than  $1/4\pi$  leads to good localization in time and frequency described as follows

$$\Delta T^2 = \int_{-\infty}^{\infty} t^2 |f(t)|^2 dt \quad (7)$$

$$\Delta F^2 = \int_{-\infty}^{\infty} f^2 |F(f)|^2 |df| \quad (8)$$

$$\Delta T^2 \Delta F \geq \frac{1}{4\pi} \quad 0 \leq \Delta \leq 1 \quad (9)$$

#### A. Mathematical Representation:

The mathematical description of the complete system is analyzed in this section. The whole system is modeled in matrix format with rows and column as that of subcarriers and symbols respectively. The transmitted signal with pruning input is defined as

$$S_{N \times 1} = P D \quad (10)$$

Where  $P = [P_1, P_2, P_3, \dots, P_k] \in \mathbb{C}^{N \times M K}$  with each  $P_k$  constitute of  $[p_{1,k}, p_{2,k}, \dots, p_{M,k}]$  linearly shifted QAM symbols of size  $[N \times M]$  and the combination of input sequence on spreading matrix can be represented as  $D = [D_1, \dots, D_k] \in \mathbb{C}^{M K \times 1}$  with  $D_k$  having  $[D_{1,k}, D_{2,k}, \dots, D_{M,k}]$  of size  $[M \times 1]$ ,  $N$  be the FFT size and  $k$  be the symbol index. [16]. Now after passing through the tap delay channel-A, the signal at the reception is expressed as

$$Y_{N \times 1} = H_{[N \times N]} S_{[N \times 1]} + n_{[N \times 1]} \quad (11)$$

The above described  $n$  is Gaussian white noise of zero mean and noise variance equal to  $P_n$  is added to the waveform being transmitted such that  $n \sim CN(0, P_n I_N)$ . The vector  $D_k$  is designed as duo of frequency layout matrix  $J_f \in \mathbb{C}^{M \times M/2}$  and QAM matrix of half input sequence  $is d_k \in \mathbb{C}^{M/2 \times 1}$ . And in turn frequency layout matrix is combination of scaling value  $[u]$  and DFT spread pruned matrix given by equation

$$J_f = W F_{M \times M/2} \text{diag} \{u\}$$

The use of constant vector certify that steady power is being transmitted along the horizontal element without any maximum peak power indicated by row echelon form.

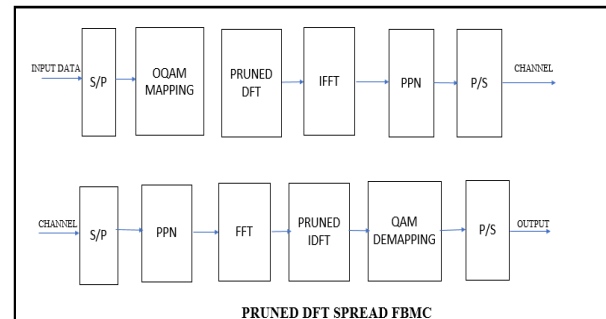


Fig. 4. Block diagram of FBMC with Pruned DFT precoded

## 5. Doubly Selective Channel TDL

In an effort to pretend diversity assets disappear, a system can be created that matches the holding line with varying timeframes. The signal from each valve can be added and the emulsion signal look like wireless swell when subject to multiway. The IRF Tapped delay channel with long rms delay is portrayed as:

$$h(t, \tau) = \sum_{i=1}^N w e_i(t) \delta(\tau - \tau_i) \quad (12)$$

Note that the impulse response  $h$  and coefficient  $c_i(t)$  varies with time  $t$ . There are  $N$  number of paths. Thus to equalize the  $N$  path model with  $N$  delay line taps are modeled [15][19]. Thus a measured single delay Minimum Mean Squared Error (MMSE) equalizer is

used for given position of subcarrier and time position k by [16],

$$e_{(l,k)} = \frac{h_{m,k}^*}{|h_{m,k}|^2 + p_n} \frac{1}{1 + \sum_{i=1}^L \frac{1}{1 + \frac{p_n}{|h_{m,k}|^2}}} \quad (13)$$

Where h is channel response, P<sub>n</sub> is the noise variance.

**Table 1.** Simulation Parameters

Radio frequency	2.5GHZ
Sub channels	256
Modulation	QAM,OQAM
FFT	256
Prototype filter	PHYDAS,Hermite
Overlay factor	4,1.56
Spacing in Frequency	15 KHZ
Medium	TDL A

## 6. Result and Discussions

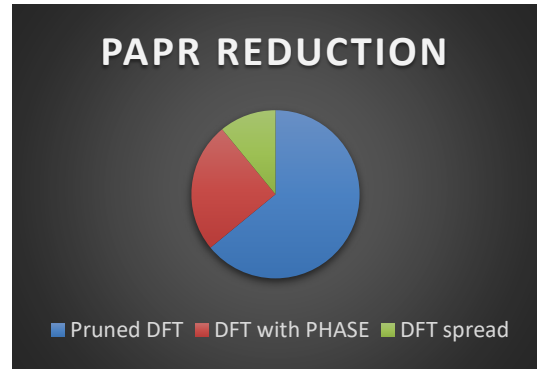
### 5.1 Peak Average Power Ratio

Fig.5,6 and 7 visualizes the PAPR by means of Complementary Cumulative Distribution Function (CCDF) for a 4,16 and 64 OQAM signal constellation and N= 256 subcarriers. As we can know as the modulation order increases the peak power will also increase. But from simulation result it is observed that even though increase in modulation order does not affect the PAPR. And also for a specific CCDF of  $1 \times 10^{-1}$ , the PAPR of the conventional system is about 12 dB where for DFT spread with pruned input, the improvement is about ~4dB. Simple DFT with FBMC just cancels the effect of IFFT symbols so produce reduction around 2 dB and it is further improved by DFT with phase factor to reduction about ~3Db. This is observed to be very enthralling that method of Pruned DFT precoding surpass PAPR of simple DFT FBMC with and without phase factor techniques. Also, one can further PAPR is reduced by exercising a CP in frequency, at the expenditure of a limited spectral effectiveness. By using OQPSK the PAPR can also be subtracted but has a dicker in spectral effectiveness.

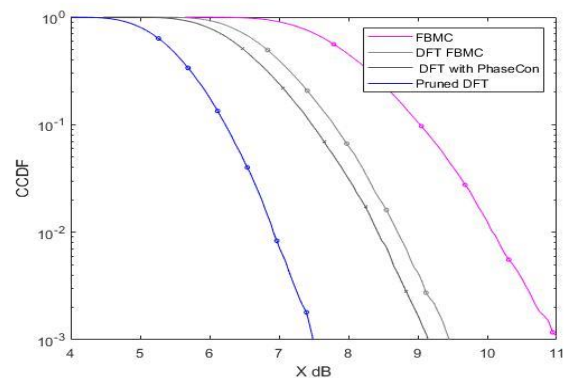
### 5.2 BIT ERROR RATE.

Figure 7 visualizes the contraction performances of bit error rate of conventional FBMC with other DFT techniques. As ratio of Signal to noise power is affected due to this nonlinearity in transmit signal power, disturbs the bit error rate and increase the cost of error. Therefore, from the computation of signal power corresponds to noise power against number of received bit error from 0 to 15 dB it is inferred this method paved less error rate as compared

with generated bit even with the changes in Peak power reduction and restore BER as like as traditional method.



**Fig.5.** Results and findings



**Fig.6.** Improvement of PAPR in 4 OQAM FBMC

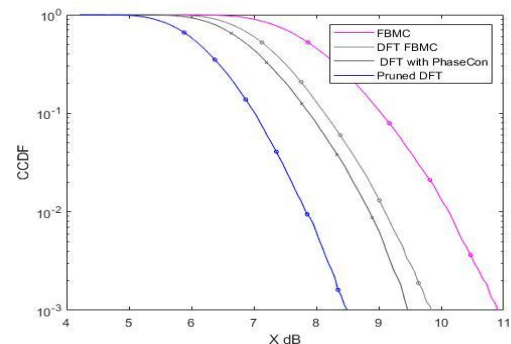


**Fig.7.** Improvement of PAPR in 16 OQAM FBMC

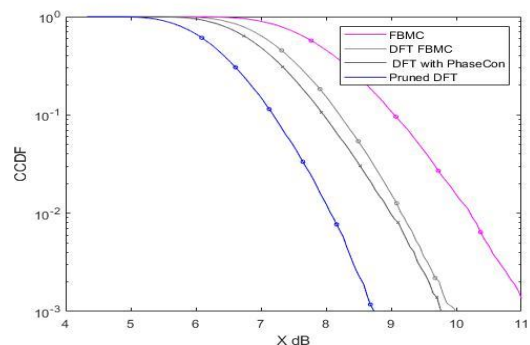


**Fig.8.** Improvement of PAPR in 64 OQAM FBMC

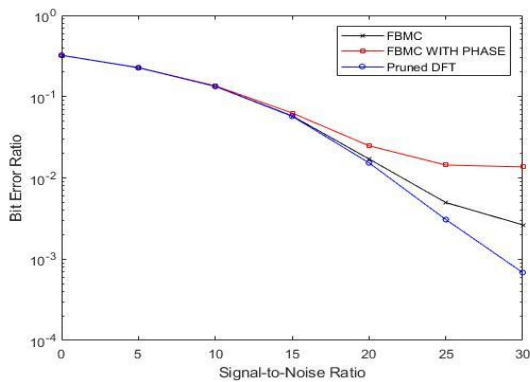


**Fig. 9.** BER of reduction techniques with conventional FBMC

## 6. Conclusion

Firstly, the simple DFT gradually decreases the power of highest peak marginally by cancelling the IFFT effect. From all these simulated result and theoretical analysis, it is inferred that the effect of DFT will definitely reduce the crest power of the generated signal. Further addition to DFT will result in reduction of PAPR. Then in addition to optimum phase factor with four version of generated waveform and the selecting the one among them leads to further peak power improvement. Finally, DFT with precoding method adapt the row echolean of layout matrix form for contraction of crest power by assuming the CSI is known. To make it more constraint scaling factor is also employed. Thus peak power to average power ratio is reduced leading to linear working of power amplifier. Further the system is analyzed in one of the time and frequency selective channel named TDL-A channel model becomes simple to analyse. Equalization is done in terms of one tap MMSE. Hence it robust to the fading effect and Dropller effect. Finally, by also employing Hermite filter rather than PHYDAS good time and frequency localization is obtained. Reduced transmit power leads to good BER rate too. Latency and complexity remains as same as conventional method. Thus the DFT spread with pruned input FBMC is the optimum contradiction method provides high date rate, good frequency localization, less spectral leakages in addition to that the proposed method has less PAPR nearly 4 dB reduced and also gradual increase of PAPR reduction Thus this contended waveform modulation technique can be used for 5G networks.

## Conflict Of Interest

The authors declare no conflict of interest

## Authors Contributions

All authors had approved the final version

## References

[1] S. Prasetyo and T. Suryani, "Implementation of Predistorter for HPA Nonlinearity Mitigation on OQAM FBMC System," 2022, IEEE 12th Annual Computing and Communication Workshop and Conference (CCWC), pp. 1036-1042, doi: 10.1109/CCWC54503.2022.9720842

[2] L. Li, X. Chen, L. Xue, D. Hu and Z. Zhang,

"Improved Interference Cancellation Method in FBMC/OQAM system on PAPR reduction," 2021 IEEE International Conference on Computer Science, Electronic Information Engineering and Intelligent Control Technology (CEI), 2021, pp. 790-794, doi: 10.1109/CEI52496.2021.9574528.

- [3] D. Kong, X. Zheng, Y. Yang, Y. Zhang and T. Jiang, "A Novel DFT-Based Scheme for PAPR Reduction in FBMC/OQAM Systems," in *IEEE Wireless Communications Letters*, vol. 10, no. 1, pp. 161-165, Jan. 2021, doi: 10.1109/LWC.2020.3024179
- [4] S. Alshami, "Performance Analysis of OFDMA, UFMC, and FBMC for Optical Wireless Communication," 2021 1st International Conference on Emerging Smart Technologies and Applications (eSmarTA), 2021, pp. 1-4, doi: 10.1109/eSmarTA52612.2021.9515739.
- [5] X. Zhang *et al.*, "SSB Pruned DFT-Spread FBMC Signal with Low PAPR in Direct-Detection PONs," in *IEEE Photonics Journal*, vol. 12, no. 3, pp. 1-13, June 2020, Art no. 7903113, doi: 10.1109/JPHOT.2020.2993075
- [6] S. Jang, D. Na and K. Choi "Comprehensive Performance Comparison Between OFDM-based and FBMC-based Uplink Systems," International Conference on Information Networking (ICOIN), 2020, pp. 288-292, doi: 10.1109/ICOIN48656.2020.9016425.
- [7] X. Cheng, D. Liu, W. Shi, Y. Zhao, Y. Li and D. Kong, "A Novel Conversion Vector-Based Low-Complexity SLM Scheme for PAPR Reduction in FBMC/OQAM Systems," in *IEEE Transactions on Broadcasting*, vol. 66, no. 3, pp. 656-666, Sept. 2020, doi: 10.1109/TBC.2020.2977548.
- [8] H. M. Abdel-Atty, W. A. Raslan and A. T. Khalil, "Evaluation and Analysis of FBMC/OQAM Systems Based on Pulse Shaping Filters," in *IEEE Access*, vol. 8, pp. 55750-55772, 2020, doi: 10.1109/ACCESS.2020.2981744.
- [9] S. Lv, J. Zhao, L. Yang and Q. Li, "Genetic Algorithm Based Bilayer PTS Scheme for Peak-to-Average Power Ratio Reduction of FBMC/OQAM Signal," in *IEEE Access*, vol. 8, pp. 17945-17955, 2020, doi: 10.1109/ACCESS.2020.2967846.
- [10] N. A. Mohamed Al Harthi, Z. Zhang and S. Choi, "FBMC-OQAM PAPR Reduction Schemes," 2020 International Conference on Information and Communication Technology Convergence (ICTC), 2020, pp. 148-150, doi: 10.1109/ICTC49870.2020.9289244.
- [11] D. Na and K. Choi, "DFT Spreading-Based Low PAPR FBMC with Embedded Side Information," in *IEEE Transactions on Communications*, vol. 68, no. 3, pp. 1731-1745, March 2020, doi: 10.1109/TCOMM.2019.2918526.
- [12] M. A. Aboul-Dahab, M. M. Fouad and R. A. Roshdy, "Generalized Discrete Fourier Transform for FBMC Peak to Average Power Ratio Reduction," in *IEEE Access*, vol.7, pp. 81730-81740, 2019, doi: 10.1109/ACCESS.2019.2921447

- [13] K. Choi, "Alamouti Coding for DFT Spreading-Based Low PAPR FBMC," in *IEEE Transactions on Wireless Communications*, vol. 18, no. 2, pp. 926-941, Feb. 2019, doi: 10.1109/TWC.2018.2886347.
- [14] S. Ramavath, B. Ramavath and R. Akhil, "Theoretical Analysis of the PAPR for DFT Spreading Based FBMC," *2019 4th International Conference on Recent Trends on Electronics, Information, Communication & Technology (RTEICT)*, 2019, pp. 1285-8143, doi: 10.1109/RTEICT46194.2019.9016886.
- [15] G. -R. Barb, M. Oteteanu, G. Budura and C. Balint, "Performance Evaluation of TDL Channels for Downlink 5G MIMO Systems," *2019 International Symposium on Signals, Circuits and Systems (ISSCS)*, 2019, pp. 1-4, doi: 10.1109/ISSCS.2019.8801790.
- [16] R. Nissel and M. Rupp, "Pruned DFT-Spread FBMC: Low PAPR, Low Latency, High Spectral Efficiency," in *IEEE Transactions on Communications*, vol. 66, no. 10, pp. 4811-4825, Oct. 2018, doi: 10.1109/TCOMM.2018.2837130
- [17] D. Na and K. Choi, "Low PAPR FBMC," in *IEEE Transactions on Wireless Communications*, vol. 17, no. 1, pp. 182-193, Jan. 2018, doi: 10.1109/TWC.2017.2764028
- [18] U. Boyapati and S. C. Prema, "Reduction of PAPR in FBMC: A Comparative Analysis," *2018 IEEE Recent Advances in Intelligent Computational Systems (RAICS)*, 2018, pp. 84-88, doi: 10.1109/RAICS.2018.8634899.
- [19] T. Blazek, M. Ashury, C. F. Mecklenbräuker, D. Smely and G. Ghiaasi, "Vehicular channel models: A system level performance analysis of tapped delay line models," *2017 15th International Conference on ITS Telecommunications (ITST)*, 2017, pp. 1-8, doi: 10.1109/ITST.2017.7972222
- [20] Sahin, R. Yang, E. Bala, M. C. Beluri and R. L. Olsen, "Flexible DFT-S-OFDM: Solutions and Challenges," in *IEEE Communications Magazine*, vol. 54, no. 11, pp. 106-112, November 2016, doi: 10.1109/MCOM.2016.1600330CM.
- [21] Sahin, I. Guvenc and H. Arslan, "A Survey on Multicarrier Communications: Prototype Filters, Lattice Structures, and Implementation Aspects," in *IEEE Communications Surveys & Tutorials*, vol. 16, no. 3, pp. 1312-1338, Third Quarter 2014, doi: 10.1109/SURV.2013.121213.00263.
- [22] G. Berardinelli, F. M. L. Tavares, T. B. Sorensen, P. Mogensen and K. Pajukoski, "Zero-tail DFT-spread-OFDM signals," *2013 IEEE Globecom Workshops (GC Wkshps)*, 2013, pp. 229-234, doi: 10.1109/GLOCOMW.2013.6824991
- [23] F. Li, J. Yu, Z. Cao, J. Xiao, H. Chen and L. Chen, "Reducing the peak-to-average power ratio with companding transform coding in 60 GHz OFDM-ROF systems," in *Journal of Optical Communications and Networking*, vol. 4, no. 3, pp. 202-209, March 2012, doi: 10.1364/JOCN.4.000202.
- [24] T. Ihalainen, A. Viholainen, T. H. Stitz, M. Renfors and M. Bellanger, "Filter bank based multi-mode multiple access scheme for wireless uplink," *2009 17th European Signal Processing Conference*, 2009, pp. 1354-1358.
- [25] Y. G. Li and G. L. Stuber, *Orthogonal Frequency Division Multiplexing for Wireless Communications*. New York, NY, USA: Springer, 2006